Theoretical Study of Lithium-Doped Polycyclic Aromatic Hydrocarbons

Hiroki Ago, Koji Nagata, Kazunari Yoshizawa, Kazuyoshi Tanaka, and Tokio Yamabe*

Department of Molecular Engineering, Graduate School of Engineering, Kyoto University, Sakyo-ku, Kyoto 606-01

Institute for Fundamental Chemistry, 34-4 Takano-Nishihiraki-cho, Sakyo-ku, Kyoto 606

(Received February 3, 1997)

The interactions between carbon layers and lithium atoms are described with a semiempirical molecular orbital method in order to clarify the Li storage mechanism in amorphous carbon (a-C) materials used in Li ion rechargeable batteries. The general electronic and geometric structures of Li-doped a-C materials are investigated using ovalene ($C_{32}H_{14}$) as a model carbon structure. The following results are obtained. (i) The intercalation of Li atoms proceeds preferentially up to the C_6Li configuration, followed by the absorption of Li atoms on the surface of the carbon layer. (ii) The adsorption of Li atoms can occur even on the nearest neighbor site and can form Li cation clusters commensurate with the carbon lattice. (iii) Li atoms located at the acene-edge sites are more stable than those at the phenanthrene-edge sites. This result suggests that the acene-edge structure is favorable for carbon anode materials. (iv) Substitution of the carbon skeleton by heteroatoms such as boron and nitrogen is not effective for Li storage.

In recent years, carbon materials have been extensively studied for application to anode materials of lithium ion rechargeable batteries.[1—5] Carbon materials do not lead to the formation of lithium dendrite, which is one of the most serious problems in applying Li-based materials to the electrode of a battery. A high capacity, high output voltage, good reversibility, and long cycle life, which are essential properties for high-performance rechargeable batteries, can be realized by using carbon materials prepared from appropriate starting materials and heat treatment.[3,5]

There are two main approaches for the formation of carbon anode materials with high electrochemical performance. One approach is to use highly graphitic carbon materials, in which Li atoms can intercalate the carbon layers up to the so-called C_6Li state indicated in **1** (Scheme 1). In this state, Li atoms are located over every three benzene ring.[6] The theoretical capacity of the fully intercalated graphite is 372 mA h g^{-1}.[3] Highly graphitic carbons exhibit several advantages, such as a constant output voltage and good reversibility. The preparation of highly graphitic carbon materials is technologically not so difficult; it is prepared by heat treatment at high temperature (2000—3000 °C) to achieve a high crystallinity.

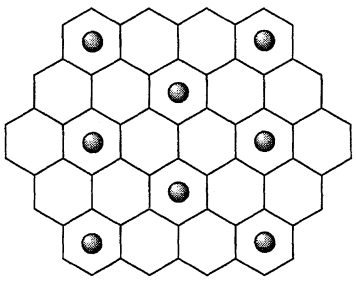

1

Scheme 1.

Another approach is to utilize amorphous carbon (a-C) materials, which have been investigated extensively because their capacity is higher than that of graphite. a-C materials can be classified into two main categories, i.e., soft (graphitizable) and hard (non-graphitizable) carbon materials. The electrochemical properties of such a-C materials as well as highly graphitic carbons were recently reviewed by Dahn et al.[3]

A remarkably high capacity of 1100 mA h g^{-1}, which corresponds to the C_2Li state, has been reported in polyacenic semiconductor (PAS) materials prepared from heat treatment of phenol–formaldehyde resin at relatively low temperature (600—800 °C).[2,7] The study of the Li storage mechanism and the electronic structure of such highly doped a-C materials is very interesting not only from engineering but also from scientific viewpoints. However, when using a-C materials for Li ion rechargeable batteries, it has been suggested that there are disadvantages such as Li loss in the first charging-discharging cycle and a large hysteresis in electrode potential vs. capacity profile.[2,3]

The Li storage mechanism of a-C materials has been studied extensively, but is still a subject of controversy, due to their disordered structures, which are still not clear at present. A lot of experiments have been performed to explain the unique characteristics of Li-doped a-C materials. For instance, an interesting model that Li atoms are located over every benzene ring (C_2Li) has been proposed on the basis of ^7Li NMR measurements.[8] On the other hand, the high capacity of a-C materials was explained by the presence of three kinds of Li species, i.e., intercalation between the

layers, adsorption on the surface, and deposition in the edge of the carbon layer(s).[9] On the basis of a linear relationship between capacity and [H]/[C] molar ratio, a Li atom has been suggested to form a covalent bond with a peripheral carbon atom of a-C materials.[3,10]

In spite of a large amount of work, three is no satisfactory answer for the Li storage mechanism in a-C materials. Thus, it is important to investigate the electronic and geometric structures of Li-doped a-C materials from a theoretical viewpoint. To the best of our knowledge, there have been a few theoretical studies on the Li-doping mechanism.[11—14] We study the electronic and geometric structures of the Li-doped carbon material as a function of the number of Li atoms, using a molecular orbital (MO) method. Throughout this paper, ovalene ($C_{32}H_{14}$) molecules are used as a model structure of a-C. Though actual a-C materials include a number of defects such as sp^3-hybridized carbon atoms and functional groups, we think the present model can help in understanding the Li-doping mechanism and in the design of high performance a-C materials, because a major component of a-C materials is a polycyclic aromatic hydrocarbon.[15]

In the next section, details of calculations are described, followed by results and discussion which consists of six items.

1. Energetically favorable positions of Li dopants are investigated using an ovalene sheet doped with two-Li atoms.
2. Differences of two types of Li-doping models, intercalation and adsorption models, are examined by employing two ovalene sheets.
3. Intercalation model is examined as a function of interlayer distance of two ovalene sheets.
4. A new adsorption model is proposed using an ovalene sheet doped with an even number of Li ions.
5. Undoping process of amorphous carbon materials is discussed from the molecular orbital aspect.
6. Effects of substitution of carbon atoms for the hetero atoms, e.g., as boron and nitrogen, are investigated.

In the final section, results are summarized.

Method of Calculation

MO calculations were performed with the modified neglect of diatomic overlap (MNDO) method.[16] This method has been extensively employed for organolithium compounds because a systematic study on methyllithium[17] suggested that the MNDO method gives quite reasonable results. Moreover, the MNDO method has been successfully applied to structural analyses of organolithium compounds.[18] We used the GAUSSIAN 94 MO program package[19] to perform MO calculations.

As a model carbon structure, ovalene was employed in this study, as mentioned above, because molecules possessing D_{6h} symmetry such as coronene and circumcoronene, which seem to be appropriate for model structures of a-C materials, are technically difficult to treat, due to their degenerate MOs.[12] In addition, ovalene possesses two types of edge structures, as will be mentioned later. The geometry of ovalene was fixed within D_{2h} symmetry; all the C–C and C–H bonds were fixed as 1.40 and 1.08 Å, respectively, and all the bond angles as 120 °C. The [H]/[C] molar ratio, which determines various properties of a-C materials, is 0.44 for ovalene. This value corresponds to that of PAS materials which are heat-treated at 530 °C.[20] All the systems calculated contain an even number of Li atoms because of the restricted Hartree–Fock (RHF) method used in this study. Favorable positions for dopant Li were analyzed for various structures in terms of heat of formation (ΔH_f). The net charge of Li atoms was obtained from Mulliken's population analysis.[21]

Results and Discussion

1. Favorable Li Positions. Let us first examine favorable positions for dopant Li, using two-Li models with different geometric structures. Figure 1 indicates six kinds of Li positions calculated. Geometry optimization for the distance (d) between Li and the ovalene layer only was carried out, except for a coplanar model as indicated in Fig. 1(f). Only in this coplanar model was the distance between the Li

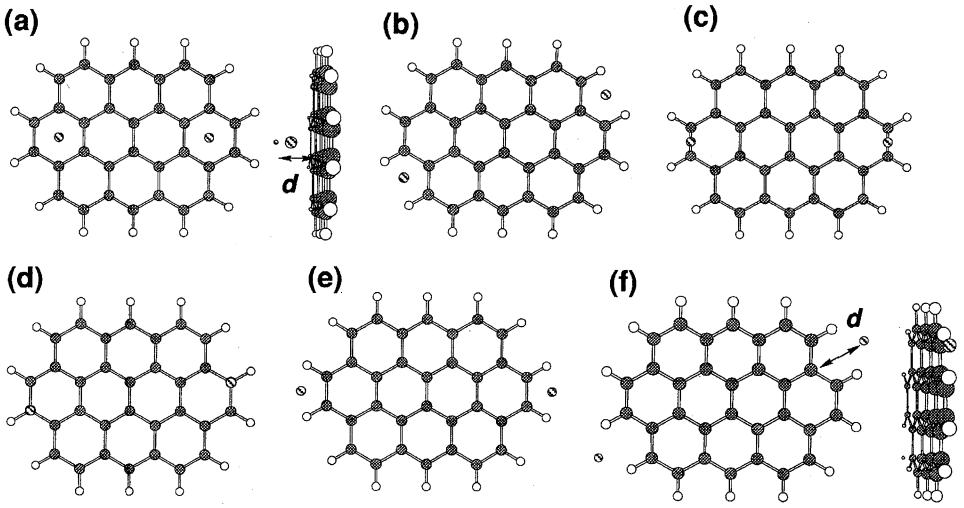

Fig. 1. Configurations of two-Li-doped ovalene systems. The Li atoms are located over (a) center of benzene ring (ring-over site), (b) acene-edged (acene-edge site), (c) C–C bond (bond-over site), (d) C atoms (atom-over site), and (e) phenanthrene-edge (phenanthrene-edge site). The vertical distance, d, between the Li and the ovalene sheet was optimized. In configuration (f), the Li atoms are located on the same plane with ovalene and the distance between the edge carbon was optimized.

Table 1. Calculated Results of Two-Li Doped Ovalene Systems

Location of Li atoms[a)]	Heat of formation/eV	Relative energy[b)] eV	Optimized distance, d (Å)	Li charge[c)]
(a) Ring-over site	6.934	0.0	1.867	1.05
(b) Acene-edge site	7.635	0.701	1.713	1.00
(c) Bond-over site	7.939	1.005	2.023	0.98
(d) Atom-over site	7.980	1.046	2.017	0.98
(e) Phenanthrene-edge site	8.842	1.908	1.701	0.97
(f) Coplanar site	9.724	2.790	2.841[d)]	1.03

a) Locations of lithium atoms are shown in Fig. 1. b) Positive value indicate unstable state. c) Determined by Mulliken population analysis. d) Distance from the carbon atom indicated by the arrow in Fig. 1.

and the edge carbon atom optimized. The heats of formation, relative energies, optimized distances, d, and net charges of Li are summarized in Table 1. The Li atoms are found to be completely ionized as a form of Li^{1+} at this doping level ([Li]/[C]=6 %). The calculated overestimation of Li charge may be attributed to Mulliken's population analysis, since this analysis partitions the two centered atomic orbital (AO) bond population equally for different atoms.[21] However, this does not cause a serious problem in the analyses throughout this paper. The electrons transferred from the Li atoms to the ovalene sheet are located mainly on the 2pπ-AOs of the carbons near Li atoms.

From Table 1 we can see several interesting characteristics, as indicated below. (i) The position over the center of a benzene ring (ring-over site) is the most favorable site for dopant Li, as is well-known in the first stage of the lithium–graphite intercalation compound (Li–GIC).[6] (ii) For Li ions, the acene-edge site, indicated in Fig. 1(b), is more favorable than the phenanthrene-edge site, indicated in Fig. 1(e). This can be derived from the difference in the number of carbon atoms around the Li ion, because the negatively charged carbon atoms can stabilize the Li ion electrostatically. There is in general large LUMO (the lowest unoccupied molecular orbital) amplitude in the acene-edge site, so that the Li ion is greatly stabilized in this region. (iii) The position over the C–C bond (bond-over site) is slightly more favorable for Li than the site just over the carbon atom (atom-over site). These relative energies per Li atom are approximately 0.5 eV compared with that of the most favorable ring-over site. Note that this valued is qualitatively consistent with ab initio values, 0.3—0.4 eV, obtained for one Li atom sandwiched between two circumcoronene layers.[13] (iv) The coplanar model[9] is unrealistic because the stabilization effect through electrostatic attraction between carbon π-electrons and a Li cation is quite weak.

Some of the results described above can be understood qualitatively by electrostatic interactions between the delocalized π-electrons on the ovalene sheet and a positively charged Li nucleus (attractive) and also the 1s electrons remaining in Li^{1+} (repulsive), though the 1s electrons are not explicitly included in the semiempirical MNDO method. It is found that the favorable Li position is a direct consequence of electrostatic interactions.

The optimized distance d shown in Table 1 is 1.867 Å at the ring-over position (Fig. 1(a)), and this value agrees fairly well with the observed distance of the first stage Li–GIC (d changes from 1.675 to 1.853 Å as a result of Li intercalation).[6] On the other hand, the d values at the bond-over and atom-over positions (indicated in Figs. 1(c) and 1(d), respectively) are larger than 2 Å, which shows that these types of interactions are not attractive. Thus, the ring-over site is energetically favored for dopant Li.

To get more information about favorable positions for dopant Li, the change in ΔH_f was examined as a function of Li···Li distance by using the models indicated in Fig. 2. We fixed one Li atom on a terminal benzene ring and moved another Li atom from the phenanthrene- or acene-edge site to the nearest neighboring benzene ring. We kept the Li···ovalene nonbonded distance to be 2 Å. As we see in Fig. 2(a), the position of Li at site B is much more stable than the phenanthrene-edge site, A. It is important to note that the migration of Li from site A to site B has no cost of activation energy. This suggests that Li can enter very easily between the carbon layers. Closer approach to the fixed Li makes the system energetically unstable, due to the electrostatic repulsion between the Li ions. Although Li can be located on site C, the occupation of the nearest neighbor site D is very difficult due to strong electrostatic repulsion.

The migration from the acene-edge site was also investigated, as shown in Fig. 2(b). We see that acene-edge site A is quite favorable for Li, compared with phenanthrene-edge site; interestingly, the stability at site A is at the same level as that of ring-over site B. However, when site C is occupied by dopant Li, strong electrostatic repulsion work, and as a consequence, the system becomes energetically unstable. From the great stability at site B in Fig. 2(b), we can see that the C_6Li configuration can be formed without electrostatic repulsion. An observed remarkable decrease in the Li charge at site D in Fig. 2(a) and site C in Fig. 2(b) (ca. +0.75) would be derived from a decrease in the electrostatic repulsion between the Li ions.

2. Intercalation and Adsorption Models. Having described favorable positions for dopant Li, in this section we describe the properties of model systems consisting of two dopant Li and two ovalene sheets. Figure 3 shows two model structures and their ΔH_f. One model (Fig. 3(a)) has two dopant Li inside the two layers, and the other (Fig. 3(b)) has two Li atoms outside the layers; we call them intercalation

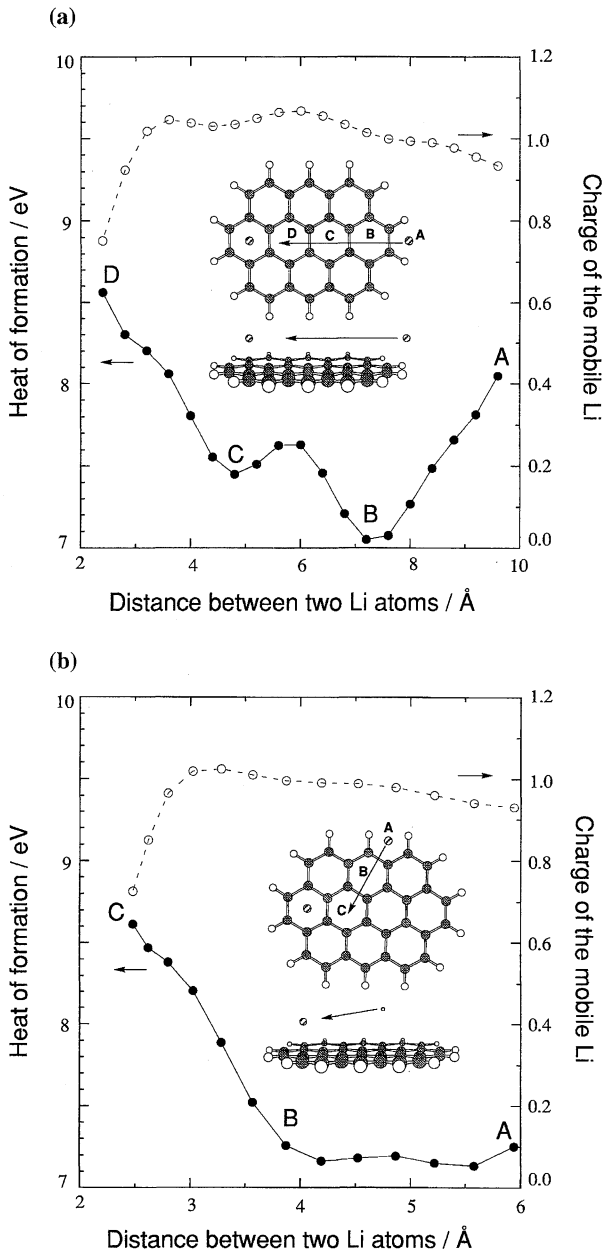

Fig. 2. The energy profiles of the two-Li-doped systems with regard to the Li position. One Li atom is fixed at the center of the ring, and another Li atom is moved from (a) the phenanthrene-edge, and (b) the acene-edge. The heat of formation (closed circle) and the charge of the moved Li (open circle) are plotted as a function of Li–Li distance.

and adsorption models, respectively. A great stabilization energy is found in the intercalation model compared with the adsorption one, due to the structure of Li ions sandwiched by two negatively charged ovalene sheets. Thus, in an actual doping process in graphite or a-C materials, we think that the adsorbing Li dopants preferentially migrate into carbon layers and, after complete occupation of intercalating sites, the adsorbing Li dopants remain. An observation[22] that in disordered coke carbon materials a change in interlayer distance is larger in a low doping stage would support this result.

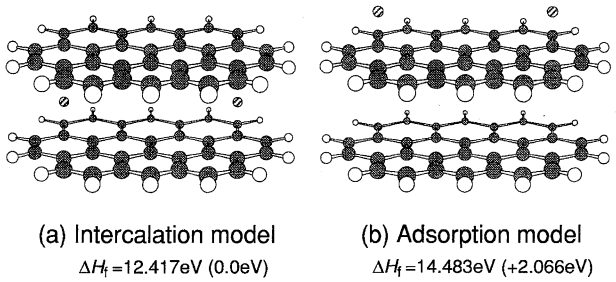

Fig. 3. Comparison of the heat of formation of the two Li atoms in (a) intercalation and (b) adsorption models. In the parenthesis the relative energy is indicated.

The most interesting problem is how many Li atoms can coexist with the two ovalene sheets. The difference in the energy profiles between intercalation and adsorption models was studied by using the two models shown in Figs. 4(a) and 4(b), where the interlayer distance is fixed at 4.0 Å and all the Li···ovalene distances are kept at 2.0 Å. Assuming first the C_6Li configuration, we examined energy profiles with respect to the positions of newly added two Li dopants in the intercalation and adsorption models. In these models, [Li]/[C] ratio is 22 %, which is larger than that of C_6Li state (17%). When two Li atoms intercalate from the phenanthrene-edges simultaneously (Fig. 4(a)), the ΔH_f of the system increases largely after passing the peripheral C–C bond. This result shows that the ratio of intercalating Li atoms cannot exceed that of the C_6Li configuration. In this process, the Li charge of approximately 1.0 does not decrease, so that this destabilization is clearly a consequence of the electrostatic repulsion between Li dopants.

Since newly added Li atoms are fully ionized, strong electrostatic repulsion works and prevents the occupation at the nearest neighbor site. We find that the charges of intercalating Li are independent of the number of adsorbing Li as well as of the number of intercalating Li atoms (ten Li atoms intercalate between two ovalene sheets, and all the Li atoms are fully ionized). In this way the C_2Li configuration within the carbon layers cannot be expected from our calculations. The fact that the C_2Li state with an intercalation structure can be formed only under an extreme condition of 50 kbar and 280 °C[23] supports our result. The transferred electrons are found to spread on the carbon atoms of two ovalene sheets, especially on the carbons near the Li atoms.

We look in detail at the change of ΔH_f in Fig. 4(a). The calculated local minimum of ΔH_f at distance of 0.8 Å suggests the possible existence of loosely trapped Li ions at the phenanthrene-edge site. This is an interesting result, because it shows that Li ions can exist in the periphery of carbon planes after the so-called C_6Li sites, indicated in **1**, are fully occupied. The occupation at the acene-edge site sandwiched by the two carbon layers can occur preferentially even after the C_6Li configuration is completed, since Li trapped at the acene-edge site is more stable than that at the phenanthrene-edge site, as mentioned above. Thus, we think that the observed high doping level in a-C materials can be ascribed to such local trapping sites in the peripheral region of carbon

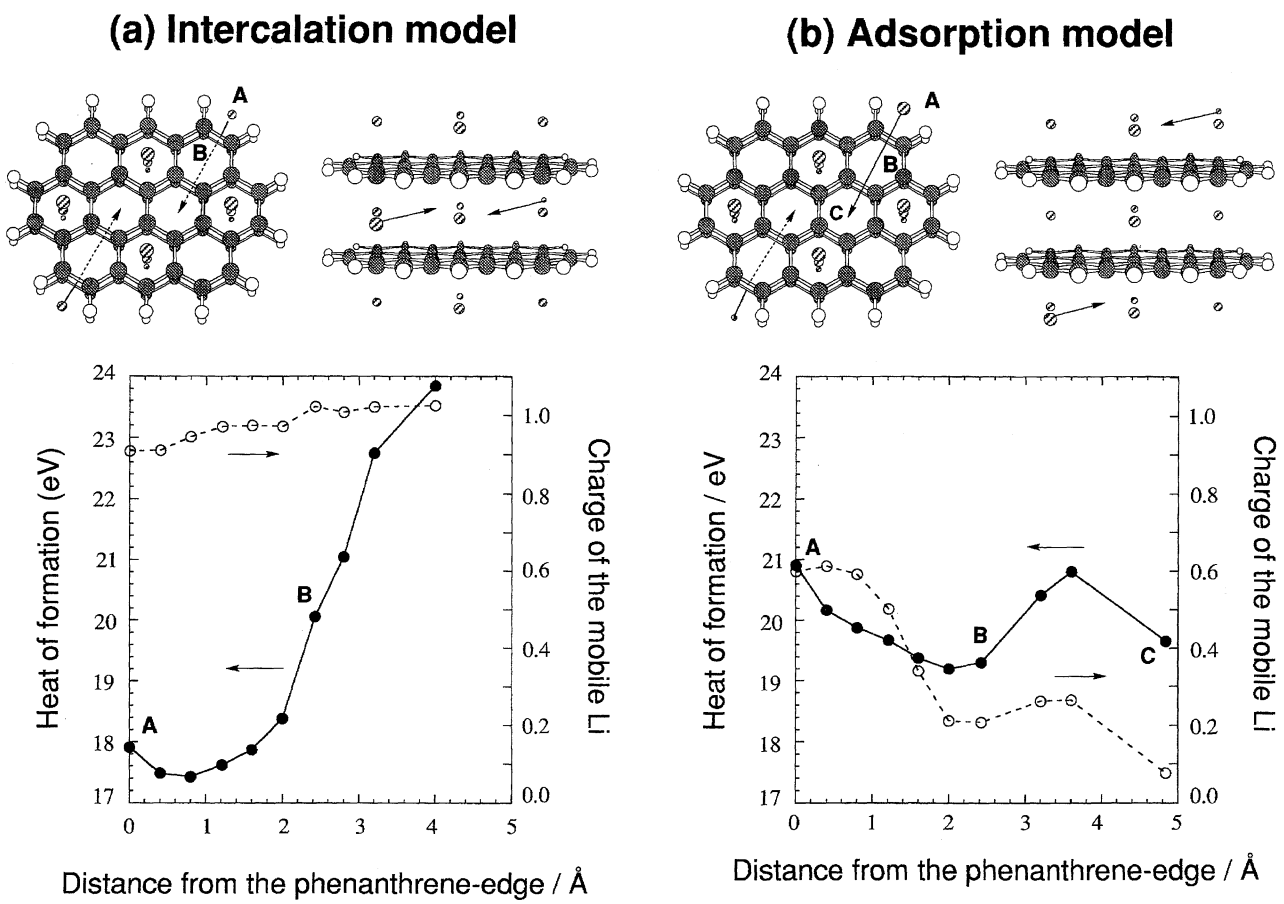

Fig. 4. Comparison of the energy profiles of (a) intercalation and (b) adsorption. In the 12 Li doped systems (4 and 8 Li atoms intercalate and adsorb, respectively), extra two Li atoms (a) intercalate and (b) adsorb simultaneously as indicated by the arrow. Closed and open circles show the heat of formation and charge of the extra Li, respectively.

planes.

Let us next look at the adsorption model, shown in Fig. 4(b). Two local minima are clearly seen in the ΔH_f curve (at B and C sites), after passing the outer C–C bond. Thus, site B and site C can be occupied by dopant Li. It is noteworthy that the charge of the newly added Li is less positive than that of intercalating Li. The calculated Li charge is in contrast to the results shown in Fig. 3, where intercalating Li ions are stabilized greatly by both the upper and lower carbon layers, which are negatively charged. The adsorption profile provides us with the possible existence of partially charged Li, and it also suggests a possibility of a higher doping level than that of the C_6Li state in graphite. We consider that these partially charged Li atoms should form molecular clusters, as discussed below. It is noted that the adsorption of Li atoms on the carbon layer was already confirmed in coroannulene.[24] Moreover, from X-ray photoelectron spectroscopy (XPS) analysis of PAS materials, it has been clarified that the Li in C_2Li state of PAS is between ionic and metallic states and is less ionic than that in C_6Li state of Li–GIC.[2,25] We suppose that the very high capacity of a-C materials can be derived from the adsorption of the carbon layer. The limit of adsorption will be discussed later in this paper.

3. Intercalation Mechanism. Intercalation over the C_6Li configuration is not realistic, as shown in the previous section, except for the edge sites. The next question is whether or not extra Li atoms can exist if D is larger than 4.0 Å. This question arises from the observed large interlayer separation in PAS materials (3.7—4.2 Å) which can contain extremely high dopant Li concentrations.[2,7,20] The relation between the interlayer separation and dopant concentration was evaluated using a model containing six Li atoms sandwiched by the two ovalene sheet, as shown in Fig. 5. The obtained energy curve suggests that there are three different regions as a function of D.

When $D > 7$ Å, the electrostatic attraction between the upper (lower) Li and the upper (lower) carbon layer are supposed to be dominant. This state can be regarded as two isolated adsorption models. In the second region of $5.4 < D < 7$ Å, the electrostatic repulsion between the upper Li and lower Li atoms are stronger than that in $D > 7$ Å. When $5.4 < D < 7$ Å, the charges of upper Li atoms are decreased as D decreases. This behavior occurs in order to reduce the electrostatic repulsion between the positively charged Li atoms. In the third region of $D < 5.4$ Å, a remarkable decrease in ΔH_f occurs with increasing Li charge. An important factor in this region is the electrostatic attraction between Li ions and two carbon layers (upper and lower), providing the most stable state though we considered in the previous section that such

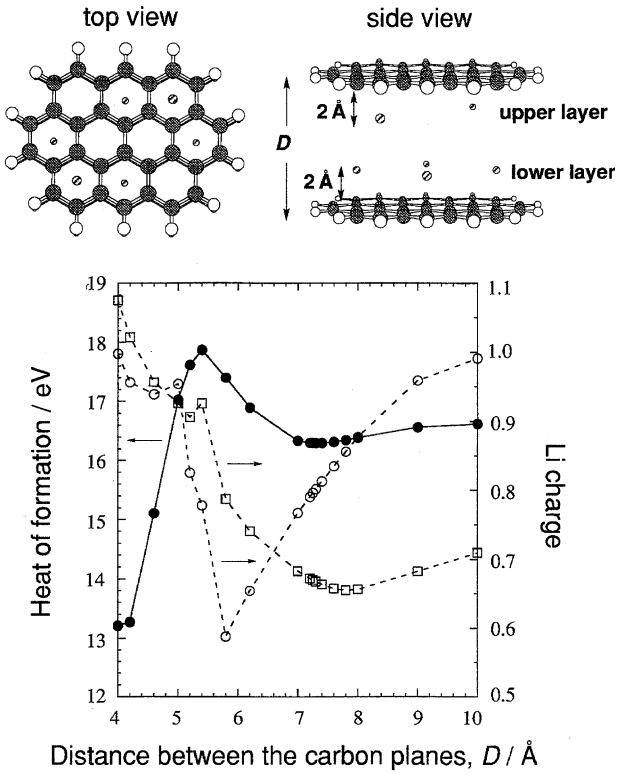

Fig. 5. The energy profile plotted vs. the interlayer distance, D, of the six-Li-intercalated system. The distance between the upper (lower) Li and the upper (lower) ovalene is fixed as 2.0 Å. The ΔH_f, the average charge of the upper and lower Li atoms are shown by closed circles, open circles, and open squares, respectively.

a state is unrealistic. It is found that separation of layers up to 7 Å is required for realization of the both-side adsorption in one layer. Since formation of such a structure is actually difficult, we think that a "house of cards" structure proposed by Dahn et al.[26] and a cyclophane-type structure proposed by us, indicated in the left and right illustrations (Scheme 2) of **2**, respectively, are more realistic models.

4. Adsorption Mechanism. Adsorption is an interesting but very complicated phenomenon. We showed in the previous section of this paper that partially charged Li atoms can be formed theoretically on the surface of the adsorption model. In Fig. 6, the most stable configurations of 2, 4, 6, and 8 Li atoms on one side of ovalene are displayed together with ΔH_f and Li charges. In two- and four-Li systems, the positions of Li atoms were fully optimized, whereas the positions in six- and eight-Li systems were fixed at the ring-over sites with $d = 2$ Å.

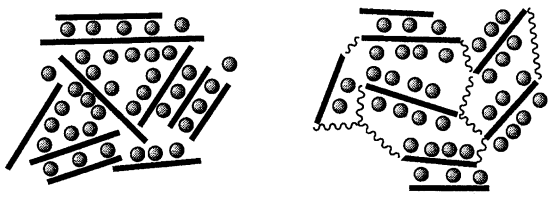

2

Scheme 2.

It is important to note that, in the four-Li system, two quite different configurations showed almost the same ΔH_f. The Li atoms in configuration A are partially charged, while those of B are fully ionized, as shown in Fig. 6. The former showed relatively long Li···ovalene distances ($d = 2.1$—2.3 Å) indicating weaker interactions between the Li atoms and the ovalene sheet. The letter has a shorter Li···ovalene distance of 1.84 Å as a consequence of strong electrostatic attractions between the Li atoms and the ovalene sheet.

These two four-Li systems are characterized well by the MO interaction diagrams shown in Fig. 7. No orbital mixing was observed in either configuration. This result shows that a dominant factor in Li-doped carbon materials is electrostatic interactions which come from a charge-transfer reaction. In configuration A, the electrons of the Li atoms occupying the next highest occupied MO (next HOMO; HOMO-1) remain unchanged after the interactions, whereas in configuration B significant electron transfer occurs from the four Li atoms to the ovalene sheet. The HOMO and (HOMO-1) of the complex in configuration B are composed of the ovalene's (LUMO+1) and LUMO, respectively. On the other hand, the (HOMO-1) of the complex in configuration A comes from the Li AOs. This remarkable difference stems from the large stability of the next HOMO in model A. In other words, in configuration A a stable Li_4^{2+} molecule is formed.

Small Li clusters with 2—30 atoms have been extensively studied[27—29] from the viewpoints of quantum size effects[30] and magic numbers.[31] From these theoretical studies, it has been clarified that planar Li clusters with 2—10 atoms favor a hexagonal structure rather than a square structure.[27] The nearest neighbor atomic distance of a neutral hexagonal cluster is 2.7—3.0 Å[27] and oxidation of such clusters is supposed to lengthen Li–Li bonds. On the basis of these calculational results, one can expect the formation of small Li (cation) clusters on carbon layer. Because the Li cluster is commensurate with the carbon lattice, only several atoms can be cohere to keep the Li–Li bond length of ca. 3 Å. Note that the Li–Li bond length of the clusters is 2.7—3.0 Å, while the distance between the nearest neighbor ring-over sites in graphite is 2.424 Å. It has been reported that Li clusters commensurate with the graphite lattice are formed on the graphite surface by injection of Li atoms.[32] Heating up to 200 °C leads to the formation of incommensurate Li clusters with diameter of ca. 100 Å.[32]

We can see coexistence of ionized and clustered Li species in the most stable six-Li system. In actual Li-doped a-C materials, Li clusters and Li ions probably coexist on the surface of the carbon layer. From ESR analyses, the spin-orbit coupling of conduction electrons was enhanced by Li doping, which suggests that the charge of dopant Li decreases as doping proceeds.[33] Although the absolute stability of the eight-Li system in Fig. 6(e) cannot be confirmed, we suppose this configuration to be unrealistic due to its commensurate structure. The deposition of Li on the carbon layer is one of the key factors which clarify the high capacity of a-C materials.

5. Discharging Mechanism. Lithium loss in the first

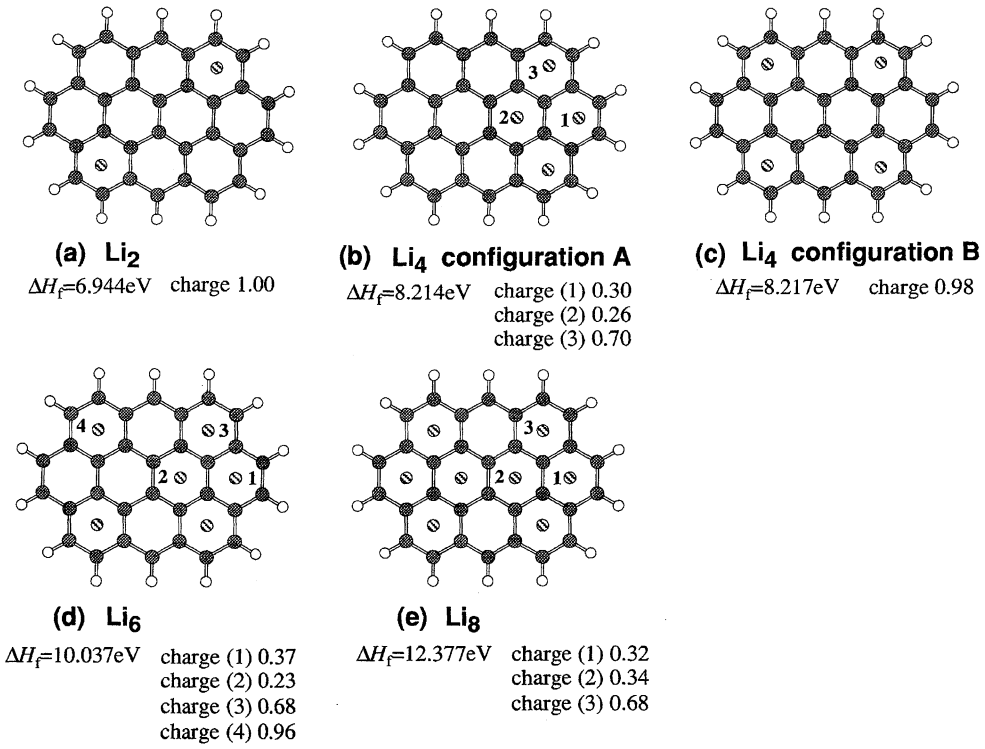

Fig. 6. The most stable configurations of 2, 4, 6, and 8 Li-atoms adsorbed ovalene system. For the two and four Li systems, the positions of Li atoms are fully optimized, while those of six and eight Li systems are fixed at the center site keeping $d = 2$ Å. In the four Li doped system, two quite different configurations, A and B, with almost the same energies were obtained.

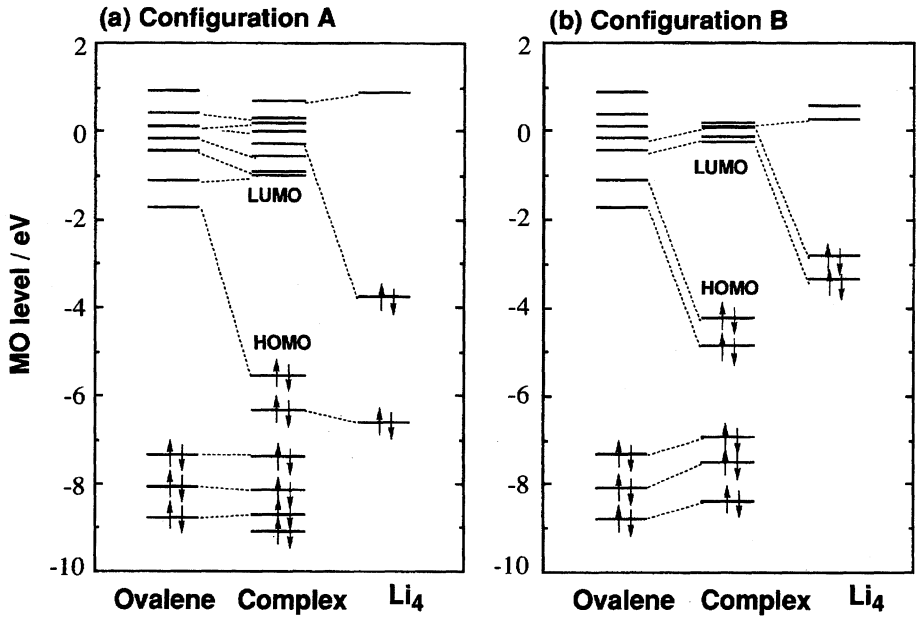

Fig. 7. Calculated MO diagram of the four Li adsorbed ovalene systems with configurations (a) A and (b) B shown in Fig. 6.

charging-discharging cycle is a serious problem in a-C materials used in Li ion rechargeable batteries because the loss reduces its reversible capacity. For instance, the irreversible capacity of PAS material is 250 mA h g^{-1} which corresponds to 29% of the total reversible capacity (850 mA h g^{-1}).[7] Discharging process is carried out by removing electrons from the negatively charged carbon materials, releasing Li^{1+} ions simultaneously into the electrolyte. Therefore Li loss would originate from the formation of still unknown Li species possessing rather high ionization potential. In this section, the reversibility of Li-doped ovalene systems is discussed on the basis of the two characteristic models indicated in Figs. 6(b) and 6(c).

In four-Li-doped ovalene system with configuration B, four 2s electrons of Li atoms transferred to ovalene, as shown in Fig. 7(b). It is therefore possible to remove the four electrons from the negatively charged ovalene, that is, all the Li^{1+} ions of configuration B can be undoped. A similar

discharging process will occur in the intercalation models, because the intercalating Li atoms are fully ionized. On the other hand, in the complex with configuration A, two 2s electrons remained on the *Li molecule* and the corresponding MO level (HOMO-1) is relatively low, as shown in Fig. 7(a). However, in this case, at least two electrons transferred to the ovalene sheet can be removed with releasing two Li^{1+} ions, resulting in two-Li adsorbed complex. We think that the highly-charged two Li atoms on site 3 of configuration A should be undoped first. As is already discussed in Fig. 2, the two remaining Li atoms will be fully ionized and separated well, followed by release of the remaining two electrons and the two Li^{1+} ions. Such a stepwise undoping process of the configuration A would cause a large hysteresis in the electrode potential vs. capacity profile.[2)]

We consider that the observed Li loss does not come from the adsorbing Li atoms nor from the intercalating Li species. As suggested in the literature,[33—35)] we think that stable states such as side-reactions of electrolytes and formation of Li–C covalent bonds are the causes of the irreversible capacity loss in Li ion rechargeable batteries.

6. Heteroatomic Effects. Let us finally look at heteroatomic effects on the doping mechanism in a-C materials. So-called heterographite, in which a part of carbon atoms are substituted by heteroatoms with various atomic ratios, i.e., BC_3, BC_2N, and C_5N, have been synthesized so far using chemical vapor deposition (CVD) techniques.[36,37)] The changes in the electronic properties of graphite caused by heteroatom substitution are of great interest for graphite-intercalation compounds.[38,39)] Several kinds of heterographites such as BC_2N have been tested as an anode material of batteries, but remarkable capacity enhancement has not been observed.[40—42)] For the design of a new type of a-C materials, it is important to examine the Li storage mecanism in heteroatomic systems from a theoretical viewpoint.

MO calculations were performed on ovalene-based heteroatomic system: $B_8C_{24}H_{14}$ and $C_{24}N_8H_{14}$. The calculated MO levels as well as those of non-substituted ovalene are shown in Fig. 8. Since a boron atom has only three valence electrons, its electron deficiency largely stabilizes the MO levels in the frontier orbital region, as indicated in Fig. 8(b). These changes in such MO levels, especially low-lying unoccupied levels, would enhance the ionization of intercalating Li atoms. On the other hand, a nitrogen atom offers two electrons for 2pπ-AO and thus destabilizes the MO levels in the frontier orbital region, as seen in Fig. 8(c). Thus, the nitrogen substitution would suppress the ionization of intercalating Li atoms.

We first examined the intercalation model for heteroatomic systems by using models similar to Fig. 4(a). The obtained energy profiles gave a results similar to the nonsubstituted system (Fig. 4(a)), which contains fully ionized intercalating Li atoms. An observed difference is the position of the local minimum of ΔH_f. The most preferred position for newly added Li was 1.6 and 0.4 Å apart from the phenanthrene-edge for the boron- and nitrogen-substituted systems, respectively, while that of the non-substituted system is 0.8

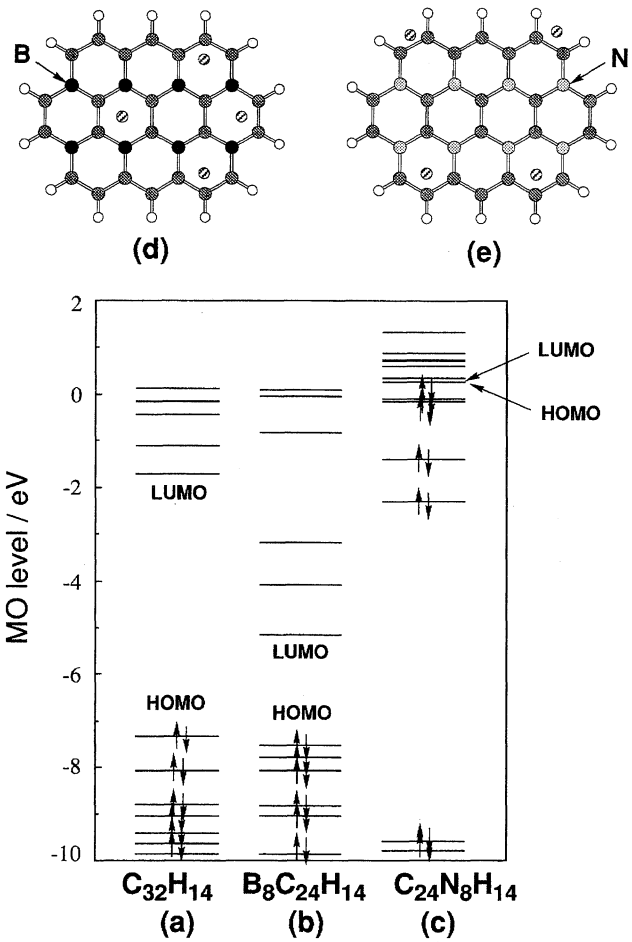

Fig. 8. Comparison of MO levels of neutral (a) ovalene, (b) boron-substituted ovalene, and (c) nitrogen-substituted ovalene systems. The positions of the heteroatoms are indicated by arrows in (d) and (e). The optimized geometry of the four-Li-doped boron-substituted system obtained from configuration A is shown in (d). In (e), the optimized geometry of the four Li doped nitrogen-substituted system obtained from configuration B is shown.

Å (see Fig. 4(a)). Thus, the local trapping site for Li described in Fig. 4(a) exists also in these heteroatomic system. Differences in the local minimum position among the non-, boron-, and nitrogen-substituted ovalenes can be explained from differences in the π-electron densities.

In case of adsorption, the commensuration of Li clusters limits the growth of larger clusters. The barriers found in the bond-over and atom-over positions would originate from the π-electrons of the carbon layer. Therefore reduction of the π-electron density occurring in boron substitution is expected to weaken the commensuration. Optimized geometries of boron-substituted ovalene of configuration A and nitrogen-substituted ovalene of configuration B are shown in Figs. 8(d) and 8(e), respectively. Although we tried to optimize the geometry of configuration A for boron-substituted ovalene, one of the Li atoms moved to the nearest neighboring ring-over site. Because the boron substitution enhances the ionization of dopant Li (+0.81—+0.98), the electrostatic repulsions be-

tween Li atoms are stronger in boron-substituted ovalene. This effect would lead to the formation of smaller Li clusters, as seen in Fig. 8(d). On the other hand, when we tried to optimize configuration B for nitrogen-substituted ovalene, two Li atoms moved out of the ovalene sheet. This is because the unoccupied levels of nitrogen-substituted ovalene are very much destabilized and as a result the system lacks enough electron affinity for housing four Li ions.

On the basis of the results obtained in these calculations, we cannot expect a higher capacity in heteroatomic a-C materials. Furthermore, odd numbers of heteroatoms will bring unpaired electron-like aromatic molecules with odd numbers of carbon atoms,[43] resulting in a covalent-like bond with Li. Hence the heteroatomic system would increase the amount of the irreversible Li atoms.

Concluding Remarks

The geometric and electronic structures of Li-doped carbon materials have been studied using ovalene as a basic carbon structure on the basis of semiempirical MO analyses. We found that the ring-over site is most favorable for dopant Li and that the activation energy for the migration of Li ion to the neighboring ring-over site is about 0.5 eV. We have examined two kinds of Li states, which are classified into intercalation and adsorption. Intercalating Li which is almost completely ionized is stabilized well by both the negatively-charged upper and lower carbon layers, which results at most in the formation of the C_6Li configuration. On the other hand, adsorbing Li atoms on the carbon layer can form small Li cation clusters concomitant with fully ionized Li atoms. Very small Li clusters are allowed to exist only on the carbon layer surface because of the restriction of the Li–Li distance of such clusters. Heteroatomic substitutions are found not to enhance a doping level from a theoretical aspect. Two major guiding principles for preparing high-capacity a-C materials are indicated below. (i) For a higher doping level, the acene-edge is more favorable than the phenanthrene-type. (ii) The interlayer distance of the carbon layers should be separated well to make Li clusters on both sides of a single carbon layer. However, it is unrealistic to separate the carbon layers up to 7 Å, as mentioned above. We think that the two models, with "house of cards" and cyclophane-type structures, indicated in **2**, are possible structures. Possible formation of Li–C chemical bond which would distort a carbon plane is of great interest and is now under study.

This work was support by a Grant-in-Aid for Scientific Research from the Ministry of Education, Science, Sports and Culture, and by the Japan Society for the Promotion of Science (JSPS-RFTF 96P00206).

References

1) T. Kitamura, T. Miyazaki, and T. Kawagoe, *Synth. Met.*, **18**, 537 (1987).

2) S. Yata, H. Kinoshita, M. Komori, N. Ando, T. Kashiwamura, T. Harada, K. Tanaka, and T. Yamabe, *Synth. Met.*, **62**, 153 (1994).

3) J. R. Dahn, T. Zheng, Y. Liu, and J. S. Xue, *Science*, **270**, 590 (1995).

4) K. Tanaka, M. Ata, H. Kimura, and H. Imoto, *Bull. Chem. Soc. Jpn.*, **67**, 2430 (1994).

5) D. Guyomard and J. M. Tarascon, *Adv. Mater.*, **6**, 408 (1994).

6) A. Hérold, "Physics of Intercalation Compounds", ed by L. Pietronero and E. Tosati, Springer, Berlin (1981).

7) S. Yata, Y. Hato, H. Kinoshita, N. Ando, A. Anekawa, T. Hashimoto, M. Yamaguchi, K. Tanaka, and T. Yamabe, *Synth. Met.*, **73**, 273 (1995).

8) K. Sato, M. Noguchi, A. Demachi, N. Oki, and M. Endo, *Science*, **264**, 556 (1994).

9) Y. Matsumura, S. Wang, and J. Mondori, *Carbon*, **33**, 1457 (1995).

10) T. Zheng, J. S. Xue, and J. R. Dahn, *Chem. Mater.*, **8**, 389 (1996).

11) C. S. Bahn, W. J. Lauderdale, and R. T. Carlin, *Int. J. Quant. Chem.*, **29**, 533 (1995).

12) K. Nagata, H. Ago, K. Yoshizawa, and T. Yamabe, "Proc. Annu. Meet. Chem. Soc. Jpn.," Tokyo, March 28—31, 1996, Abstr., No. 1PC029.

13) D. J. Hankinson and J. Almlöf, *Univ. Minnesota Supercomp. Inst. Res. Bull.*, **10**, 8 (1994).

14) P. Papanek, M. Radosavljevic, and J. E. Fischer, *Chem. Mater.*, **8**, 1519 (1996).

15) K. Tanaka, M. Ueda, T. Koike, T. Yamabe, and S. Yata, *Synth. Met.*, **25**, 265 (1988).

16) M. J. S. Dewa and W. Thiel, *J. Am. Chem. Soc.*, **99**, 4899 (1977).

17) E. Kaufmann, K. Raghavachari, A. E. Reed, and P. R. Schleyer, *Organometallics*, **7**, 1597 (1988).

18) L. A. Paquette, W. Bauer, M. R. Sivik, M. Bühl, M. Feigel, and P. R. Schleyer, *J. Am. Chem. Soc.*, **112**, 8776 (1990).

19) M. J. Frisch, J. A. Pople et al., "GAUSSIAN 94," Gaussian Inc., Pittsburgh, Pennsylvania, PA (1995).

20) K. Tanaka, T. Koike, T. Yamada, J. Yamauchi, Y. Deguchi, and S. Yata, *Phys. Rev. B*, **B35**, 8368 (1987).

21) R. S. Mulliken, *J. Chem. Phys.*, **23**, 1841 (1955).

22) Y. Mori, T. Iriyama, T. Hashimoto, S. Yamazaki, F. Kawakami, H. Shiroki, and T. Yamabe, *J. Power Sources*, **56**, 205 (1995).

23) J. Conard, V. A. Nalimova, and D. Guerard, *Mol. Cryst. Liq. Cryst.*, **245**, 25 (1994).

24) A. Ayalon, A. Sygula, P-C. Cheng, M. Rabinovitz, P. W. Rabideau, and L. T. Scott, *Science*, **265**, 1065 (1994).

25) G. K. Wertheim, P. M. Th. M. Van Attekum, and S. Basu, *Solid State Commun.*, **33**, 1127 (1980).

26) Y. Liu, J. S. Xue, T. Zheng, and J. R. Dahn, *Carbon*, **34**, 193 (1996).

27) S. Quassowski and K. Hermann, *Phys. Rev. B*, **B51**, 2457 (1995).

28) a) B. K. Rao, S. N. Khanna, and P. Jena, *Phys. Rev. B*, **B36**, 953 (1987); b) P. Jena, B. K. Rao, and R. M. Nieminen, *Solid State Commun.*, **59**, 509 (1986).

29) Y. Ishii, S. Ohnishi, and S. Sugano, *Phys. Rev. B*, **B33**, 5271 (1986).

30) J. C. Boettger and S. B. Trickey, *Phys. Rev. B*, **B45**, 1363 (1992).

31) W. D. Knight, K. Clemenger, W. A. Heer, W. A. Saunders, M. Y. Chou, and M. L. Cohen, *Phys. Rev. Lett.*, **52**, 2141 (1984).

32) Z. P. Hu and A. Ignatiev, *Phys. Rev. B*, **B30**, 4856 (1984).
33) K. Tanaka, H. Ago, Y. Matsuura, T. Kuga, T. Yamabe, S. Yata, Y. Hato, and N. Ando, *Synth. Met.*, in press.
34) H. Ago, K. Tanaka, T. Yamabe, K. Takegoshi, T. Terao, S. Yata, Y. Hato, and N. Ando, *Synth. Met.*, in press.
35) For instance, R. Fong, U. Sacken, and J. R. Dahn, *J. Electrochem. Soc.*, **137**, 2009 (1990).
36) J. Kouvetakis, R. B. Kaner, M. L. Sattler, and N. Bartlett, *J. Chem. Soc., Chem. Commun.*, **1986**, 1758.
37) A. W. Moore, S. L. Strong, G. L. Doll, M. S. Dresselhaus, I. L. Spain, C. W. Bowers, J. P. Issi, and L. Piraux, *J. Appl. Phys.*, **65**, 5109 (1989).
38) J. P. LaFemina, *J. Phys. Chem.*, **94**, 4346 (1990).
39) P. Saalfrank, W. Rümler, H. U. Hummel, and J. Ladik, *Synth. Met.*, **52**, 1 (1992).
40) a) M. Ishikawa, T. Nakamura, M. Morita, Y. Matsuda, S. Tsujioka, and T. Kawashima, *J. Power Sources*, **55**, 127 (1995); b) M. Morita, T. Hanada, H. Tsutsumi, Y. Matsuda, and M. Kawaguchi, *J. Electrochem. Soc.*, **139**, 1227 (1992).
41) B. M. Way and J. R. Dahn, *J. Electrochem. Soc.*, **141**, 907 (1994).
42) W. J. Weydanz, B. M. Way, T. Buuren, and J. R. Dahn, *J. Electrochem. Soc.*, **141**, 900 (1994).
43) K. Yoshizawa, K. Okahara, T. Sato, K. Tanaka, and T. Yamabe, *Carbon*, **32**, 1517 (1994).